DOR: 20.1001.1.25383620.2022.6.2.8.1

Review Article

Several Horizontal and Vertical Cracks in a Piezoelectric Rectangular Plane

R. Bagheri*

Department of Mechanical Engineering, Karaj Branch, Islamic Azad University, Karaj, Iran.
Received: 06 August 2022 - Accepted: 12 December 2022

Abstract

In this article, using the method of dislocation distribution and separation of variables, the mechanical fracture behavior of a thin rectangular plane made of piezoelectric material with limited length and width containing several cracks under out-of-plane mechanical and in-plane electrical loading is investigated. It is assumed that the behavior of the elastic medium is linear and the surfaces of the cracks are smooth. At first, the governing equations of the problem are solved according to the boundary conditions, and then the components of stress and electrical displacement in the body without cracks under external loading at the hypothetical crack location are presented. Then, according to Buckner's principle, the stress field obtained in the main problem and using the dislocation distribution method, the equations for analyzing the problem of several cracks are presented. By solving these equations and obtaining the distribution functions of dislocations, it is possible to obtain the stress and electric displacement factors at the tips of cracks. In this article, examples are given to verify the results and also to investigate the effects of the length, arrangement and interaction between the cracks on the field intensity factors.

Keywords: Piezoelectric, Rectangular Plane, Screw Dislocation, Multiple Cracks, Field Intensity Factors.

1. Introduction

Stress analysis in the vicinity of defects is necessary as the first step in the design process, and for this, the state of stress intensity at the tips of cracks is investigated. In the problems of fracture mechanics, using the dislocation method for stress analysis in limited and unlimited mediums is a common method. From a mathematical point of view, the crack can be considered as a set of dislocations, and using the superposition principle, the effects of the relative movement of the edges of the crack relative to each other, and as a result, the stress intensity factor can be calculated. Piezoelectric materials are a class of smart materials that have the ability to communicate between the fields of electricity and mechanics. Based on this property, the application of mechanical stress causes electrical displacement in the material, and in the same way, placing the material under an electric field causes mechanical strain. Due to the lack of valuable studies on the problems of cracks in the piezoelectric rectangular plane, this issue can be investigated. At first, a review of the research done in this field is done. Dislocation is one of the sources of internal stress in the body, and Volterra [1] was one of the first to define dislocation. Zhang [2] obtained the dynamic stress intensity factor in a finite rectangular plane containing a pair of edge cracks under out-of-plane mechanical loading.

*Corresponding author
Email address: r.bagheri@kiau.ac.ir

The stress field in a rectangular sheet containing an eccentric crack under the mode III of fracture mechanics was studied by Ma and Zhang [3].
They determined the stress intensity factor for the crack tip and investigated the geometrical parameters. Zhou et al. [4] investigated the stress field in the vicinity of two parallel cracks perpendicular to the edges of the isotropic strip. In this problem, the cracks are symmetrical with respect to the central line of the strip and are subjected to out-of-plane loading. Stress analysis in an isotropic layer weakened by two parallel cracks located on the centerline of the strip under out-of-plane shear was performed by Zhou and Ma [5]. Li and Wu [6] studied the problem of moving crack under out-of-plane loading between two layers of dissimilar piezoelectric material. To solve the problem, they used integral cosine Fourier transformation and obtained the effects of crack moving speed on stress intensity factor. Singular stress and electric field for a rectangular plane made of piezoelectric materials under out-of-plane mechanical and in-plane electrical loading were analyzed by Lee and Kwon [7]. They used the piezoelectric linear theory in this study. In another article by Kwon and Lee [8], the stress and electric displacement intensity factrors as well as the energy release rate under electromechanical transient load in a rectangular plane made of piezoelectric ceramic materials containing a central crack were investigated. The problem of interaction between repeated cracks at the interface of several elastic layers under out-of-plane loading is

presented by Wang and Gross [9]. In this study, the number of layers is arbitrary and cracks can be located in any of the layers. They used the Fourier series and converted the combined boundary value problem to Hibbler singular integral equations. Lee and Kwon [10] investigated the moving crack located at the interface of a layer of ceramic piezoelectric material and two layers of orthotropic material under electrical loading. Solving was done with the help of Fourier transform and the effect of crack length, layer thickness, direction of electric loading and crack speed on dynamic stress intensity factor was investigated. Li [11] presented an analytical solution for the orthotropic strip problem containing two parallel cracks perpendicular to the edge layer. In this problem, the cracks are symmetrical with respect to the central line of the layer and are subjected to out-of-plane loading. Li and Lee [12] performed an electroelastic stress analysis for a crack with an arbitrary position in a rectangular plane made of piezoelectric ceramics under out-of-plane mechanical and in-plane electrical loading. The problem of a crack located at the interface between two dissimilar orthotropic layers under out-of-plane loading was done by Li [13] and the stress intensity factors were obtained analytically. Zhou et al. [14] presented the solution of the piezoelectric/piezomagnetic material problem under out-of-plane mechanical and in-plane electromagnetic loading, and the relationships between electric displacement, magnetic field and stress field near the crack tips were determined. The out-of-plane deformation of the orthotropic layer containing several cracks and cavities was obtained by the Faal et al. [15]. In this research, the stress analysis in an orthotropic strip including a Volterra-type dislocation was carried out, and by using the dislocation solution, the integral equations for a layer weakened by cracks and cavities under out-of-plane loading were determined. Solving the problem of functionally graded electromagnetoelastic rectangular plane containing a moving crack under out-of-plane mechanical and in-plane electromagnetic load was done by Qin et al. [16]. The effect of geometry, crack moving speed and piezoelectric material constants on the stress intensity factor was investigated. Stress analysis of electromagnetic elastic material containing a coin-shaped crack and two parallel cracks under out-of-plane mechanical and in-plane electromagnetic transient loading was performed by Zhong and Zhang [17]. The dynamic analysis of fracture mechanics of a homogeneous electromagnetoelastic rectangular sheet containing a crack was obtained by Zhang [18] and in this paper, Schmidt's method was used. Fall et al. [19] solved the problem of fracture mechanics in an isotropic rectangular plane weakened by several cracks and cavities with different boundary conditions under out-of-plane loading. They used the method of separation of variables to solve the dislocation problem of Volterra type. Bagheri et al. [20,21] investigated the layer made of piezoelectric and electromagnetoelastic material with functionally properties. They presented the effect of crack length and speed and material parameters on field intensity coefficients. Ayatollahi et al. [22] investigated a half plane made of electromagnetic elastic material with a functionally graded property containing several moving cracks. In another study, Bagheri et al. [23] investigated the piezoelectric layer reinforced with a coating of orthotropic material with functionally graded properties under static out-of-plane mechanical and in-plane electrical loading. Stress analysis of a rectangular plane with functionally behavior containing several straight and curved cracks under out-of-plane loading based on the dislocation distribution method was presented by Faal and Dehghan [24]. They studied the effect of crack length and the interaction between them on the stress intensity factor.

In this article, stress analysis is performed on a rectangular plane made of piezoelectric material containing several cracks under anti-plane mechanical and in-plane electrical load. The dislocation method and the method of separation of variables have been used to obtain the governing equations of the problem. The equations are solved according to the boundary conditions and the multi-quantity of displacement and electric potential on the dislocation line and stress and electric displacement fields are provided. Then, using the dislocation distribution method, the equations for analyzing the problem of several cracks in a rectangular plane are obtained. At the end, examples are given to validate the results and investigate the effects of length, arrangement and interaction between cracks on field intensity factors.

2. Basic relationships governing piezoelectric rectangular plane

In this problem, out-of-plane mechanical loading and in-plane electrical loading in x and y plane are considered. As a result, the displacement components in the direction of the x and y axes are zero and there are only displacement components perpendicular to the plane. Also, the in-plane components of the electric field (E_z) are zero in the direction of the z-axis and in the direction of the x and y axes, they are represented by E_x and E_y, respectively. As a result, the following relations will exist.

$$u=0 \ , \ v=0 \ , \ w=w\ (x,y)$$
$$E_x = E_x\ (x,y), \qquad E_y(x,y) \qquad E_z=0 \qquad (1)$$

The relationships between electric field and electric potential ϕ are:

$$E_{x=} -\frac{\partial \phi}{\partial x} \qquad E_{y=} -\frac{\partial \phi}{\partial y} \tag{2}$$

For the mode III of the fracture mechanics, the components of stress and electrical displacement in the piezoelectric plane will be as follows:

$$\begin{aligned}
\sigma_{zx} &= c_{44}\frac{\partial w}{\partial x} + e_{15}\frac{\partial \phi}{\partial x} \\
\sigma_{zy} &= c_{44}\frac{\partial w}{\partial y} + e_{15}\frac{\partial \phi}{\partial y} \\
D_x &= e_{15}\frac{\partial w}{\partial x} - \varepsilon_{11}\frac{\partial \phi}{\partial x} \\
D_y &= e_{15}\frac{\partial w}{\partial y} - \varepsilon_{11}\frac{\partial \phi}{\partial y}
\end{aligned} \tag{3}$$

In relation (3) c_{44}, e_{15}, ε_{11} are elastic constant, piezoelectric constant and dielectric constant, respectively. In the absence of body forces and electric flux, the stress and Maxwell equations are:

$$\begin{aligned}
\frac{\partial \sigma_{zx}}{\partial x} + \frac{\partial \sigma_{zy}}{\partial y} &= 0 \\
\frac{\partial D_x}{\partial x} + \frac{\partial D_y}{\partial y} &= 0
\end{aligned} \tag{4}$$

By placing relations (3) in relations (4) and simplifying them, the only equations that need to be satisfied are:

$$\begin{aligned}
\frac{\partial^2 w(x,y)}{\partial x^2} + \frac{\partial^2 w(x,y)}{\partial^2 y} &= 0 \\
\frac{\partial^2 \phi(x,y)}{\partial x^2} + \frac{\partial^2 \phi(x,y)}{\partial^2 y} &= 0
\end{aligned} \tag{5}$$

To solve equations (5), the method of separation of variables is used, which for a rectangular plate containing horizontal dislocation created in the medium, displacement and electric potential are obtained as follows:
that the unknown coefficients (A_{km}, B_{km}, C_{km}, D_{km}), (E_{kn}, F_{kn}, G_{kn}, H_{kn}) as well as λ_{km}, λ_{kn} should be determined using the boundary conditions, where the indices k=1,2 refer to the lower and upper part of the dislocation, respectively.

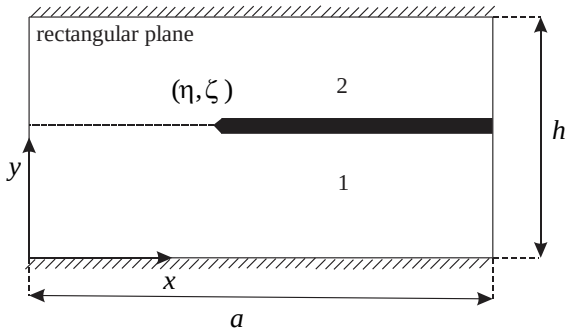

Fig. 1. Representation of dislocation in the piezoelectric rectangular plane in the state of two free edges and two fixed edges.

A rectangular quadrilateral with dimensions a×h is considered according to Fig. 1 where the edges y=0 and y=h are fixed and the other two edges are free. A screw dislocation of the Volterra type is considered with the Burgers vectors b_z and b_ϕ in the (η,ζ) coordinate, which creates a cross section in the direction of the x axis. This dislocation divides the rectangular plane into two upper and lower parts, the lower part is marked with number 1 and the upper part is marked with number 2. The boundary conditions for this problem are:

$$\begin{aligned}
&\sigma_{zx}(0,y) = D_x(0,y) = 0 \\
&\sigma_{zx}(a,y) = D_x(a,y) = 0 \\
&w(x,0) = \phi(x,0) = 0 \\
&w(x,h) = \phi(x,h) = 0
\end{aligned} \tag{7}$$

The conditions related to multi-valued displacement and electric potential due to the existence of mechanical and electric dislocation are expressed as follows:

$$\begin{aligned}
w(x,\zeta^+) - w(x,\zeta^-) &= b_z H(x-\eta) \\
\phi(x,\zeta^+) - \phi(x,\zeta^-) &= b_\phi H(x-\eta)
\end{aligned} \tag{8}$$

where H(.) is the Heaviside step function and the components of stress and electrical displacement on the dislocation line have continuity, and these conditions are:

$$\begin{aligned}
\sigma_{zy}(x,\zeta^+) &= \sigma_{zy}(x,\zeta^-) \\
D_y(x,\zeta^+) &= D_y(x,\zeta^-)
\end{aligned} \tag{9}$$

By applying boundary conditions (7) to relation (6), the following results are obtained:

$$\begin{aligned}
w(x,y) &= \sum_{m=1}^{\infty}(A_{km}\cos(\lambda_{km}x) + B_{km}\sin(\lambda_{km}x))(C_{km}\cosh(\lambda_{km}y) + D_{km}\sinh(\lambda_{km}y)) \quad k=1,2 \\
\phi(x,y) &= \sum_{n=1}^{\infty}(E_{kn}\cos(\lambda_{kn}x) + F_{kn}\sin(\lambda_{kn}x))(G_{kn}\cosh(\lambda_{kn}y) + H_{kn}\sinh(\lambda_{kn}y)) \qquad k=1,2
\end{aligned} \tag{6}$$

$$w_1(x,y)=\sum_{m=1}^{\infty}A_{1m}D_{1m}\cos(\frac{m\pi}{a}x)\sinh(\frac{m\pi}{a}y)$$

$$w_2(x,y)=\sum_{m=1}^{\infty}A_{2m}D_{2m}\cos(\frac{m\pi}{a}x)\frac{\sinh(\frac{m\pi}{a}(y-h))}{\cosh(\frac{m\pi}{a}h)}$$

$$\phi_1(x,y)=\sum_{n=1}^{\infty}E_{1n}H_{1n}\cos(\frac{n\pi}{a}x)\sinh(\frac{n\pi}{a}y)$$

$$\phi_2(x,y)=\sum_{n=1}^{\infty}E_{2n}H_{2n}\cos(\frac{n\pi}{a}x)\frac{\sinh(\frac{n\pi}{a}(y-h))}{\cosh(\frac{n\pi}{a}h)} \quad (10)$$

Using relations (10) and applying continuity conditions (9), the following relations are obtained:

$$A_{1m}D_{1m}=\frac{\cosh(\frac{m\pi}{a}(\zeta-h))}{\cosh(\frac{m\pi}{a}h)\cosh(\frac{m\pi}{a}\zeta)}A_{2m}D_{2m}$$

$$E_{1n}H_{1n}=\frac{\cosh(\frac{n\pi}{a}(\zeta-h))}{\cosh(\frac{n\pi}{a}h)\cosh(\frac{n\pi}{a}\zeta)}E_{2n}H_{2n} \quad (11)$$

On the other hand, for cosine functions, the orthogonality property can be shown as follows:

$$\int_{a_1}^{a-a_1}\cos(\frac{m\pi}{a}x)\cos(\frac{p\pi}{a}x)dx=\frac{a}{2}\delta_{mp}$$

$$\int_{a_1}^{a-a_1}\cos(\frac{n\pi}{a}x)\cos(\frac{q\pi}{a}x)dx=\frac{a}{2}\delta_{nq} \quad (12)$$

which in the obtained relations, δ_{nq}, δ_{mp} are Kronecker's deltas. With conditions (8) and using the orthogonality property expressed in relation (12), the following relations result:

$$A_{2m}D_{2m}=\frac{2b_z}{m\pi}\frac{\sin(\frac{m\pi}{a}\eta)\cosh(\frac{m\pi}{a}h)\cosh(\frac{m\pi}{a}\zeta))}{\sinh(\frac{m\pi}{a}\zeta)} \quad 0\le y\le\zeta$$

$$E_{2n}H_{2n}=\frac{2b_\phi}{n\pi}\frac{\sin(\frac{n\pi}{a}\eta)\cosh(\frac{n\pi}{a}h)\cosh(\frac{n\pi}{a}\zeta))}{\sinh(\frac{n\pi}{a}\zeta)} \quad \zeta\le y\le h \quad (13)$$

By inserting relations (13) into relations (11), the following relations can be obtained:

$$A_{1m}D_{1m}=\frac{2b_z}{m\pi}\frac{\sin(\frac{m\pi}{a}\eta)\cosh(\frac{m\pi}{a}(\zeta-h))}{\sinh(\frac{m\pi}{a}h)}$$

$$E_{1n}H_{1n}=\frac{2b_\phi}{n\pi}\frac{\sin(\frac{n\pi}{a}\eta)\cosh(\frac{n\pi}{a}(\zeta-h))}{\sinh(\frac{n\pi}{a}h)} \quad (14)$$

Finally, by using relations (13) and (14) in relations (10), the mechanical displacement field and electric potential are obtained as follows:

By having the field of mechanical displacement and electric potential and placing it in relations (3), the components of stress and electric displacement are obtained as follows.

$$w_1(x,y)=\frac{2b_z}{m\pi}\sum_{m=1}^{\infty}\frac{\sin(\frac{m\pi}{a}\eta)\cosh(\frac{m\pi}{a}(\zeta-h))}{\sinh(\frac{m\pi}{a}h)}\cos(\frac{m\pi}{a}x)\sinh(\frac{m\pi}{a}y) \quad 0\le y\le\zeta$$

$$w_2(x,y)=\frac{2b_z}{m\pi}\sum_{m=1}^{\infty}\frac{\sin(\frac{m\pi}{a}\eta)\cosh(\frac{m\pi}{a}\zeta)}{\sinh(\frac{m\pi}{a}h)}\cos(\frac{m\pi}{a}x)\sinh(\frac{m\pi}{a}(y-h)) \quad \zeta\le y\le h$$

$$\phi_1(x,y)=\frac{2b_\phi}{n\pi}\sum_{n=1}^{\infty}\frac{\sin(\frac{n\pi}{a}\eta)\cosh(\frac{n\pi}{a}(\zeta-h))}{\sinh(\frac{n\pi}{a}h)}\cos(\frac{n\pi}{a}x)\sinh(\frac{n\pi}{a}y) \quad 0\le y\le\zeta$$

$$\phi_2(x,y)=\frac{2b_\phi}{n\pi}\sum_{n=1}^{\infty}\frac{\sin(\frac{n\pi}{a}\eta)\cosh(\frac{n\pi}{a}\zeta)}{\sinh(\frac{n\pi}{a}h)}\cos(\frac{n\pi}{a}x)\sinh(\frac{n\pi}{a}(y-h)) \quad \zeta\le y\le h \quad (15)$$

$$\sigma_{zx1} = -\frac{2}{a}(c_{44}b_z + e_{15}b_\phi)\sum_{n=1}^{\infty}\frac{\sin(\frac{n\pi}{a}\eta)\cosh(\frac{n\pi}{a}(\zeta-h))\sin(\frac{n\pi}{a}x)\sinh(\frac{n\pi}{a}y)}{\sinh(\frac{n\pi}{a}h)} \qquad 0 \le y \le \zeta$$

$$\sigma_{zx2} = -\frac{2}{a}(c_{44}b_z + e_{15}b_\phi)\sum_{n=1}^{\infty}\frac{\sin(\frac{n\pi}{a}\eta)\cosh(\frac{n\pi}{a}\zeta)\sin(\frac{n\pi}{a}x)\sinh(\frac{n\pi}{a}(y-h))}{\sinh(\frac{n\pi}{a}h)} \qquad \zeta \le y \le h$$

$$\sigma_{zy1} = \frac{2}{a}(c_{44}b_z + e_{15}b_\phi)\sum_{n=1}^{\infty}\frac{\sin(\frac{n\pi}{a}\eta)\cosh(\frac{n\pi}{a}(\zeta-h))\cos(\frac{n\pi}{a}x)\cosh(\frac{n\pi}{a}y)}{\sinh(\frac{n\pi}{a}h)} \qquad 0 \le y \le \zeta$$

$$\sigma_{zy2} = \frac{2}{a}(c_{44}b_z + e_{15}b_\phi)\sum_{n=1}^{\infty}\frac{\sin(\frac{n\pi}{a}\eta)\cosh(\frac{n\pi}{a}\zeta)\cos(\frac{n\pi}{a}x)\cosh(\frac{n\pi}{a}(y-h))}{\sinh(\frac{n\pi}{a}h)} \qquad \zeta \le y \le h$$

$$D_{x1} = -\frac{2}{a}(c_{44}b_z - \varepsilon_{11}b_\phi)\sum_{n=1}^{\infty}\frac{\sin(\frac{n\pi}{a}\eta)\cosh(\frac{n\pi}{a}(\zeta-h))\sin(\frac{n\pi}{a}x)\sinh(\frac{n\pi}{a}y)}{\sinh(\frac{n\pi}{a}h)} \qquad 0 \le y \le \zeta$$

$$D_{x2} = -\frac{2}{a}(c_{44}b_z - \varepsilon_{11}b_\phi)\sum_{n=1}^{\infty}\frac{\sin(\frac{n\pi}{a}\eta)\cosh(\frac{n\pi}{a}\zeta)\sin(\frac{n\pi}{a}x)\sinh(\frac{n\pi}{a}(y-h))}{\sinh(\frac{n\pi}{a}h)} \qquad \zeta \le y \le h$$

$$D_{y1} = \frac{2}{a}(c_{44}b_z - \varepsilon_{11}b_\phi)\sum_{n=1}^{\infty}\frac{\sin(\frac{n\pi}{a}\eta)\cosh(\frac{n\pi}{a}(\zeta-h))\cos(\frac{n\pi}{a}x)\cosh(\frac{n\pi}{a}y)}{\sinh(\frac{n\pi}{a}h)} \qquad 0 \le y \le \zeta$$

$$D_{y2} = \frac{2}{a}(c_{44}b_z - \varepsilon_{11}b_\phi)\sum_{n=1}^{\infty}\frac{\sin(\frac{n\pi}{a}\eta)\cosh(\frac{n\pi}{a}\zeta)\cos(\frac{n\pi}{a}x)\cosh(\frac{n\pi}{a}(y-h))}{\sinh(\frac{n\pi}{a}h)} \qquad \zeta \le y \le h \tag{16}$$

3. Stress fields and electrical displacement

Stress fields and electrical displacement due to loading on the border of a rectangular piezoelectric plane without cracks with two fixed edges and two free edges

A rectangular plane made of piezoelectric material with dimensions a×h is considered according to Fig. 2 where the edges y=0 and y=h are fixed and the other two edges are free. The load applied on the border of x=0 and y=y_0 of the piezoelectric rectangle is a point force τ_0 and electric displacement D_0, which are shown by the following relations:

$$\sigma_{zx}(0,y) = \tau_0\delta(y-y_0)$$
$$D_x(0,y) = D_0\delta(y-y_0) \tag{17}$$

where δ(.) stands for the Dirac delta function.

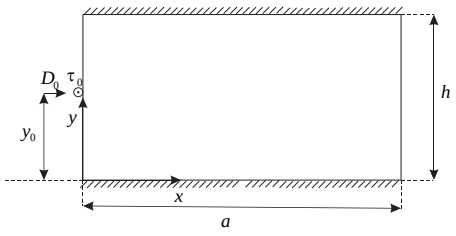

Fig. 2. Representation of rectangular piezoelectric plane under point load in the state of two fixed edges and two free edges.

The boundary conditions for this problem are:

$$\sigma_{zx}(a,y) = D_x(a,y) = 0$$
$$w(x,0) = \phi\ (x,0) = 0$$
$$w(x,h) = \phi\ \ (x,h) = 0$$
$$\sigma_{zx}(0,y) = \tau_0\delta(y-y_0)$$
$$D_x(0,y) = D_0\delta(y-y_0) \tag{18}$$

$$w(x,y)=\frac{2}{m\pi}\frac{(\varepsilon_{11}\tau_0+e_{15}D_0)}{(c_{44}\varepsilon_{11}+e_{15}^2)}\sum_{m=1}^{\infty}\frac{\sin(\frac{m\pi}{h}y_0)\cosh(\frac{m\pi}{h}(x-a))\sin(\frac{m\pi}{h}y)}{\sinh\left(\frac{m\pi}{h}a\right)}$$

$$\phi(x,y)=\frac{2}{n\pi}\frac{(e_{15}\tau_0-c_{44}D_0)}{(c_{44}\varepsilon_{11}+e_{15}^2)}\sum_{n=1}^{\infty}\frac{\sin(\frac{n\pi}{h}y_0)\cosh(\frac{n\pi}{h}(x-a))\sin(\frac{n\pi}{h}y)}{\sinh\left(\frac{n\pi}{h}a\right)} \quad (19)$$

$$\sigma_{zx}=\frac{2\tau_0}{h}\sum_{n=1}^{\infty}\frac{\sin(\frac{n\pi}{h}y_0)}{\sinh(\frac{n\pi}{h}a)}\sinh(\frac{n\pi}{h}(x-a))\sin(\frac{n\pi}{h}y)$$

$$\sigma_{zy}=\frac{2\tau_0}{h}\sum_{n=1}^{\infty}\frac{\sin(\frac{n\pi}{h}y_0)}{\sinh(\frac{n\pi}{h}a)}\cosh(\frac{n\pi}{h}(x-a))\cos(\frac{n\pi}{h}y)$$

$$D_x=\frac{2D_0}{h}\sum_{n=1}^{\infty}\frac{\sin(\frac{n\pi}{h}y_0)}{\sinh(\frac{n\pi}{h}a)}\sinh(\frac{n\pi}{h}(x-a))\sin(\frac{n\pi}{h}y)$$

$$D_y=\frac{2D_0}{h}\sum_{n=1}^{\infty}\frac{\sin(\frac{n\pi}{h}y_0)}{\sinh(\frac{n\pi}{h}a)}\cosh(\frac{n\pi}{h}(x-a))\cos(\frac{n\pi}{h}y) \quad (20)$$

By applying the boundary conditions in relations (6), the mechanical displacement field and electric potential are obtained as follows:

By having the field of mechanical displacement and electric potential and using relations (3), the components of stress and electric displacement are obtained as follows.

4. Integral equations in medium containing cracks

The dislocation solution obtained in the previous section can be used to find the field intensity afactors of a rectangular plane with two fixed edges and two free edges containing a crack under the mode III of fracture mechanics. The dislocation distribution method has been used many times by various researchers to analyze the mediums with cracks. It is assumed that the rectangular plane is weakened by N the cracks. The configuration of cracks may be described in parametric form as:

$$x_i=x_i(q)$$
$$y_i=y_i(q)$$
$$i=1,2,...,N \qquad -1\le q\le 1 \quad (21)$$

The movable orthogonal t, n coordinate system is chosen such that the origin may move on the crack while the t-axis remains tangent to the crack face. The anti-plane traction and in-plane electric displacement on the face of the i-th crack in Cartesian coordinates become:

$$\sigma_{nz}=\sigma_{zy}\cos\theta_i-\sigma_{zx}\sin\theta_i$$
$$D_n=D_y\cos\theta_i-D_x\sin\theta_i \quad (22)$$

Where θ_i is the angle between x and t-axis. The components of traction, electric displacements on the boundary of the ith crack caused by the presence of the above-mentioned distributions yield:

The kernels $K_{ij}^{11}, K_{ij}^{12}, K_{ij}^{21}$ and K_{ij}^{22} in integral Eq. (23) are coefficients of b_z and b_ϕ in stress components $\sigma_{zn} = \sigma_{zy}\cos\theta_i - \sigma_{zx}\sin\theta_i$ and electric displacements $D_n = D_y\cos\theta_i - D_x\sin\theta_i$ in Eq. (22), respectively. The left-hand side of the integral equations, having an opposite sign, is the traction and electric displacement caused by an external

$$\sigma_{nz}(x_i(q),y_i(q))=\sum_{j=1}^{N}\int_{-1}^{1}\left[K_{ij}^{11}(q,t)b_{zj}(t)+K_{ij}^{12}(q,t)b_{\phi j}(t)\right]\sqrt{\left[x_j'(t)\right]^2+\left[y_j'(t)\right]^2}\,dt$$

$$D_n(x_i(q),y_i(q))=\sum_{j=1}^{N}\int_{-1}^{1}\left[K_{ij}^{21}(q,t)b_{zj}(t)+K_{ij}^{22}(q,t)b_{\phi j}(t)\right]\sqrt{\left[x_j'(t)\right]^2+\left[y_j'(t)\right]^2}\,dt \quad (23)$$

loading on the presumed crack surfaces in the intact rectangular plane.
After calculating the dislocation density on the cracks located in the rectangular plane, relations should be provided that can be used to calculate the stress intensity factors at the tips of the cracks according to the dislocation density on the cracks. Using the definition of the dislocation density function, the opening of the crack opening and the electric potential for the jth crack, it is obtained from the following relations:

$$w_j^-(q)-w_j^+(q)=\int_{-1}^{q} b_{z\,j}(t)\sqrt{\left[x_j'(t)\right]^2+\left[y_j'(t)\right]^2}\,dt$$
$$\phi_j^-(q)-\phi_j^+(q)=\int_{-1}^{q} b_{\phi\,j}(t)\sqrt{\left[x_j'(t)\right]^2+\left[y_j'(t)\right]^2}\,dt$$
$$j=1,2,...,N \tag{24}$$

The single-valued property of displacement and electric field out of a crack surface yields the following closure conditions:

$$\int_{-1}^{1} b_{kj}(t)\sqrt{\left[x_j'(t)\right]^2+\left[y_j'(t)\right]^2}\,dt=0 \qquad k\in\{w,\phi\} \tag{25}$$

It may be shown that the kernel of integral equations (23) has only Cauchy-type singularity. Hence, the dislocation densities are of the forms:

$$b_{kj}(t)=\frac{f_{kj}(t)}{\sqrt{1-t^2}}, \qquad -1\le t\le 1,\ k\in\{w,\phi\} \tag{26}$$

The bounded function $f_{kj}(t)$ may be acquired by making use of the numerical method. The fields intensity factors for embedded cracks are:
For brevity, the details of the derivation of field intensity factors are not mentioned in here.

5. Numerical Results and Discussion

Using the obtained out-of-plane dislocation solution, examples of a rectangular plane made of piezoelectric material containing several cracks are presented. This part of the article is divided into two main parts. In the first part, examples are given to verify the results and relationships, and in the second part, examples are given to show the effect of crack length and interaction between cracks, point load application location and piezoelectric material constants on stress and electrical displacementintensity factors. In this article, the properties of piezoelectric material is considered as follows:

$$c_{44}=4.4\times10^{10}\,\frac{N}{m^2} \qquad e_{15}=5.8\,\frac{C}{m^2}$$
$$\varepsilon_{11}=5.64\times10^{-9}\,\frac{C}{Vm^2}$$

In the following examples, the quantity in order to make the field intensity factor dimensionless is defined as:

$$K_{0M}=\tau_0/\sqrt{l}, \qquad K_{0D}=(\tau_0 d_{110})/(e_{150}\sqrt{l})$$

where l represents the half-length of the crack. Additionally, $\lambda_D=D_0e_{150}/\tau_0d_{110}$ is a representation of the electro-mechanical coupling factor. Moreover, unless otherwise stated, a piezoelectric rectangular plane is under point-load anti-plane mechanic shear τ_0 and in-plane electric loading D_0. Fig. 3. shows the dimensionless stress intensity factor K_M/K_{0M} in terms of dimensionless distance X_c/a. y_c is the vertical distance of the crack center from the bottom edge of the rectangular plane and U and L represent the upper and lower tips of the crack, respectively.

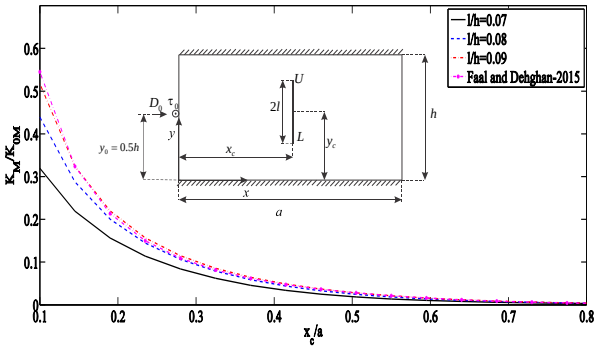

Fig. 3. Variations of dimensionless mechanical stress intensity factor in terms of X_c/a under point load.

$$(K_{III}^{m})_{Li}=\frac{c_{44}}{2}\left[\left[x_i'(-1)\right]^2+\left[y_i'(-1)\right]^2\right]^{\frac{1}{4}}f_{mi}(-1)+\frac{e_{15}}{2}\left[\left[x_i'(-1)\right]^2+\left[y_i'(-1)\right]^2\right]^{\frac{1}{4}}f_{pi}(-1)$$
$$(K_{III}^{m})_{Ri}=-\frac{c_{44}}{2}\left[\left[x_i'(1)\right]^2+\left[y_i'(1)\right]^2\right]^{\frac{1}{4}}f_{mi}(1)-\frac{e_{15}}{2}\left[\left[x_i'(1)\right]^2+\left[y_i'(1)\right]^2\right]^{\frac{1}{4}}f_{pi}(1)$$
$$(K_{III}^{D})_{Li}=\frac{c_{44}}{2}\left[\left[x_i'(-1)\right]^2+\left[y_i'(-1)\right]^2\right]^{\frac{1}{4}}f_{mi}(-1)-\frac{\varepsilon_{11}}{2}\left[\left[x_i'(-1)\right]^2+\left[y_i'(-1)\right]^2\right]^{\frac{1}{4}}f_{pi}(-1)$$
$$(K_{III}^{D})_{Ri}=-\frac{c_{44}}{2}\left[\left[x_i'(1)\right]^2+\left[y_i'(1)\right]^2\right]^{\frac{1}{4}}f_{mi}(1)-\frac{e_{15}}{2}\left[\left[x_i'(1)\right]^2+\left[y_i'(1)\right]^2\right]^{\frac{1}{4}}f_{pi}(1) \tag{27}$$

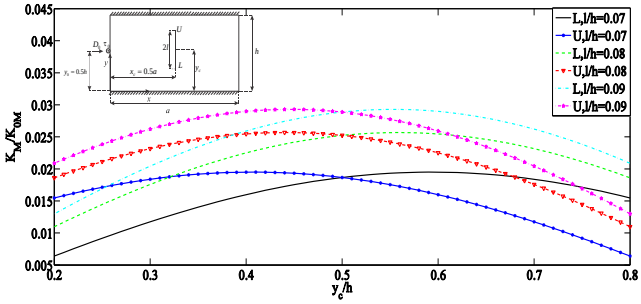

Fig. 4. Variations of dimensionless mechanical stress intensity factor in terms of y_0/h under point load.

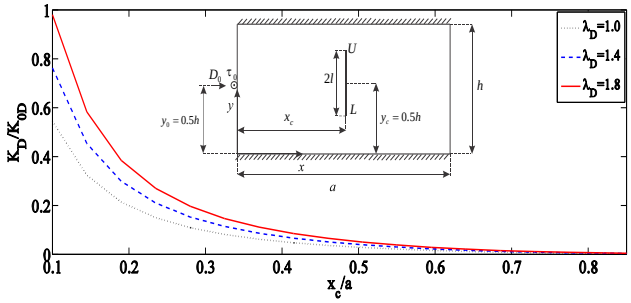

Fig. 5. Variations of KD/K0D in terms of X_c/a under point load.

This diagram shows the effect of increasing the horizontal distance of the crack center from the left edge of the rectangular plane when the point load is fixed, and it indicates that the stress intensity factor for the two crack tips decreases by moving away from the point load. It is in good agreement with the results presented by Faal and Dehghan (2015).
It is also shown in this diagram that the dimensionless stress intensity factor increases with the increase of the crack length.

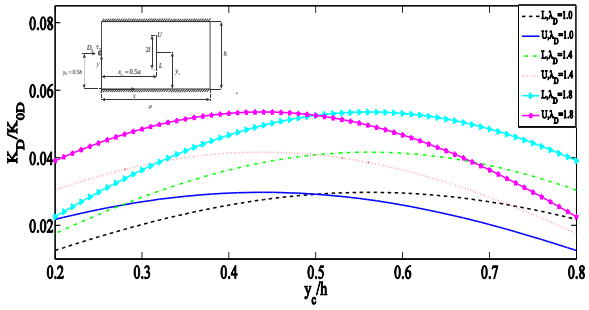

Fig. 6. Variations of K_D/K_{0D} in terms of y_c/h under point load.

Fig. 4. shows the dimensionless stress intensity factor K_M/K_{0M} in terms of the dimensionless distance y_c/h. In other words, this diagram shows the effect of increasing the vertical distance of the crack center from the bottom edge of the rectangular plane when the point load is fixed. This means that the dimensionless stress intensity factors for two crack tips increases initially as the point load approaches and then decreases as the load moves away from the crack tips, which is in good agreement with the results presented by the Faal and Dehghan in 2015. On the other hand, it can be seen that the dimensionless stress intensity factor increases with the increase of the crack length.
Fig. 5. shows the effect of the electro-mechanical coupling factor on the dimensionless electric displacement intensity factor for a vertical crack in terms of the dimensionless distance X_c/a with the dimensionless crack length (l/h=0.1). In this graph, it can be seen that with the increase in the value of X_c, the distance of the crack from the point load increases and this leads to a decrease in the displacement intensity factor, and on the other hand, on the other hand, K_D/K_{0D} increases with the increase of the electro-mechanical coupling factor.
Fig. 6 shows the effect of the electro-mechanical coupling factor on the electric displacement intensity factor for a vertical crack in terms of dimensionless distance y_c/h with dimensionless crack length l/h=0.1. This example shows that by increasing the vertical distance of the center of the crack from the bottom edge of the rectangular plane, the dimensionless displacement intensity factor at the crack tip increases initially as it approaches the point load and then decreases as it moves away from the load. It also shows that as the electroelastic dependence coefficient increases, K_D/K_{0D} increases.

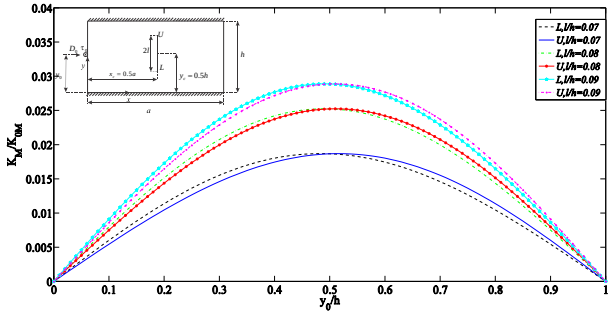

Fig. 7. Variations of mechanical stress intensity factor according to dimensionless distance y_0/h under point load.

Fig. 7. shows the effect of increasing the dimensionless crack length on the dimensionless mechanical stress intensity factor for a vertical crack in terms of dimensionless distance y_0/h and different dimensionless crack lengths l/h=0.07, 0.08, 0.09. This diagram shows that with the increase of the vertical distance of the point load from the bottom edge of the rectangular plane y_0, the dimensionless stress intensity factor at the crack tip increases initially as the point load approaches the crack tip and then as it moves away from the point load of the crack tip decreases. It also shows that the dimensionless stress intensity factor K_M/K_{0M} increases with the increase of the crack length.

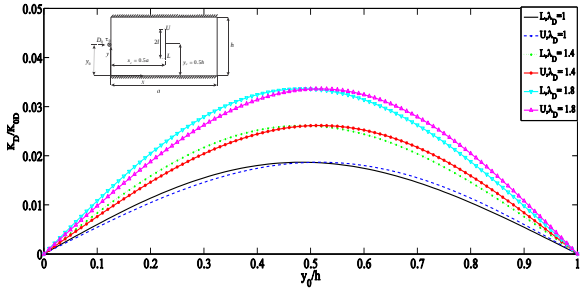

Fig. 8. Variations of electric displacement stress intensity factor according to dimensionless distance y0/h under point load.

Fig. 8. shows the effect of the electroelastic dependence coefficient on the electric displacement intensity factor for a vertical crack in terms of the dimensionless distance y_0/h with the dimensionless crack length l/h=0.07. As shown in the figure below, with the increase of the vertical distance of the point load from the bottom edge of the rectangular plane, the dimensionless displacement intensity factor at the crack tip increased initially as it approached the point load and then decreased as it moved away from the load. It also shows that as the electroelastic dependence coefficient increases, K_D/K_{0D} increases.

Fig. 9. shows the effect of increasing the dimensionless crack length on the dimensionless stress intensity factor for a vertical crack for y_0/h=0.1,0.2,0.7. As it is evident from Fig. 9., with the increase of the crack length, the dimensionless stress intensity factor K_M/K_{0M} increases and similar to the previous graphs, it is obvious that as the point load approaches the crack tip, K_M/K_{0M} increases.

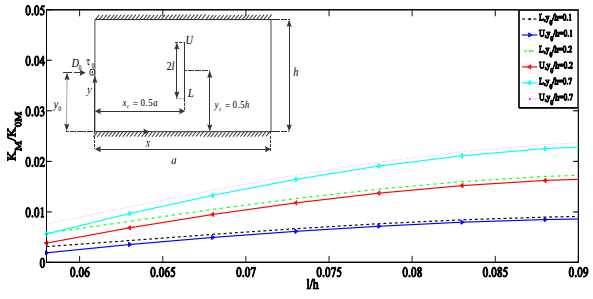

Fig. 9. Variations of K_M/K_{0M} according to dimensionless distance l/h under point load.

Fig 10 shows the effect of increasing the distance of the point load from the bottom edge of the rectangular plane on the dimensionless mechanical stress intensity factor for two vertical and horizontal cracks with different dimensionless lengths l/h= 0.2, 0.18. In this diagram, the vertical crack tips are examined. This diagram shows that the arrangement of two cracks has a significant effect on changes in the mechanical stress intensity factor because the two cracks may have protective or anti-protective effects.

As can be seen, it is expected that the stress intensity factor at the crack tip L_1 will be higher at the beginning due to being close to the point load, and this situation will change when passing through the center of the crack, but due to the protective effect, the opposite happens.

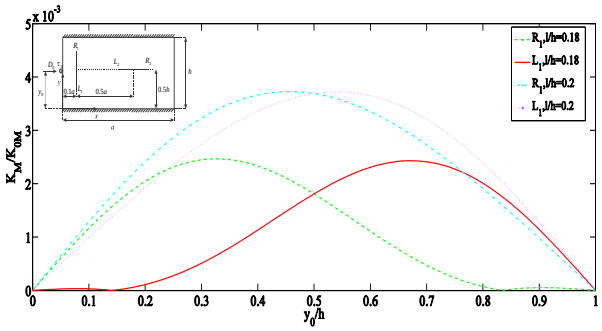

Fig. 10. Variations of dimensionless stress intensity factors according to dimensionless distance y_0/h under point load.

Fig. 11. shows the effect of increasing the distance of the point load from the bottom edge of the rectangular plane on the dimensionless stress intensity factor for two vertical cracks, when the horizontal distance of the second crack $X_{c\ (2)}$ changes. This example shows the effect of cracks arrangement on the stress intensity factor and it is expected that the stress intensity factor will decrease when the value of $X_{c\ (1)}$ is kept constant and $X_{c\ (2)}$ increases due to the low interaction of the two cracks, but it is reversed due to the protection effect and as the value of $X_{c\ (2)}$ increases and the two cracks move away from each other, the stress intensity factor increases.

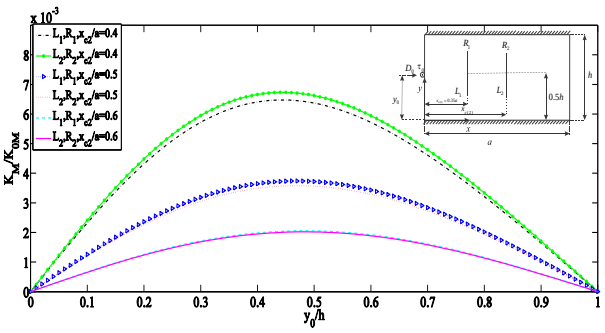

Fig. 11. Variations of dimensionless stress intensity factors according to dimensionless distance y_0/h under point load for two vertical cracks.

Fig. 12. shows the variation of dimensionless stress intensity factor K_M/K_{0M} for two horizontal cracks. As it can be seen, as the L_2R_2 crack approaches L_1R_1, the interaction between the two cracks increases and on the other hand, the L_2R_2 crack is closer to the point load, and these two factors increase the K_M/K_{0M}.

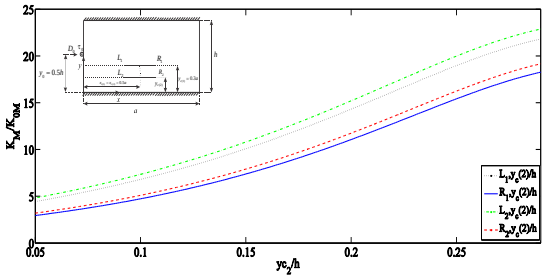

Fig. 12. Variations of dimensionless stress intensity factors according to dimensionless distance y_{c2}/h under point load for two horizontal cracks.

6. Conclusion

The mode III fracture problem of a piezoelectric rectangular plane weakened by multiple cracks under concentrated anti-plane mechanical and in-plane electrical loading is studied. The solution of screw dislocation in a piezoelectric rectangular plane is obtained by using the integral transform technique. The unknown dislocation density on cracks surfaces was calculated through solving a set of integral equations of Cauchy singular type. The solutions are obtained in series expansion forms which may be considered as Green's functions in a piezoelectric rectangular plane possessing several cracks. The technique of Green's function provides the ability to analyze multiple cracks having any smooth configuration. Finally, from the solved examples, the following results are obtained:

1. Increasing the length of the crack causes an increase in the intensity of mechanical stress and electrical displacement.
2. Increasing or decreasing the distance of the crack from the point load increases or decreases the field intensity coefficients, respectively.
3. Increasing the coefficient of electroelastic dependence increases the electric displacement intensity factor.
4. The point load application location or in other words the distance and proximity of the point load to the crack tip will decrease or increase the field intensity factors, respectively.
5. The distance between two horizontal and parallel cracks may have protective and anti-protective effect.

References

[1] V. Volterra, "Sur Pequilibre Des Carps Elastiques Multiplement Connexes"Annales ScientifiquesDel, Ecole Normal Superiure, Paris, Series3, Vol.24, (1907), 401.
[2] X. S. Zhang, Eng. Fract. Mech., Vol. 35, (1990), 1037.
[3] S. W. Ma, L. X. Zhang, Eng. Fract. Mech., Vol.40, (1991), 1.
[4] Z. G. Zhou, B. Wang, S. Y. Du, Mech. Res. Commun., Vol. 25, .（1998） , 183.
[5] Z. G. Zhou, L. Ma, Mech. Res. Commun., Vol.26, (1999), 437.
[6] Li, X.F., X. F. Wu, Int. J. Eng. Sci., Vol. 38, (2000), 1219.
[7] K. Y. Lee, S. M. Kwon, Int. J. of Solids and Struct., Vol. 37, (2000), 4859.
[8] S. M. Kwon, K. Y. Lee, Eur. J. Mech. A/Solids, Vol. 20, (2001), 457.
[9] Y. S. Wang, D. Gross, Int. J. Solids Struct., Vol. 38, (2000), 4631.
[10] J. S. Lee, K. Y. Kwon, J. H, Eur. J. Mech. A/Solids, Vol. 21, (2002), 483.
[11] X. F. Li, Mech. Res. Commun., Vol. 30, (2003), 365.
[12] X. F. Li, K. Y. Lee, Eur. J. Mech. A/S0lids, Vol. 23, (2004), 645.
[13] X. F. Li, Appl. Math. Comput., Vol. 163, (2005), 961.
[14] Z. G. Zhou, L. Z. Wu, B. Wang, Arch. Appl. Mech., Vol. 74, (2005), 526.
[15] R. T. Faal, S. J. Fariborz and H. R. Daghyani, J. Mech. Mater. Struct., Vol.1, (2006), 1097.
[16] Q. H. Qin, Y. L. Kang and K. Q. Hu, Eng. Fract. Mech., Vol. 74, (2007), 751.
[17] X. C. Zhong and K. Zhang, Eur. J. Mech. A/Solids, Vol. 29, (2010), 242.
[18] P. W. Zhang, Int. J. Solids Struct., Vol. 48, (2011), 553.
[19] R. T. Fall, M. Daliri and A. S. Milani, Int. J. Solids Struct., Vol. 48, (2011), 661.
[20] R. Bagheri, M. Ayatollahi and S. M. Mousavi, Math. Mech.Solids, Vol. 30, (2015), 1.
[21] R. Bagheri, M. Ayatollahi and S. M. Mousavi, Appl. Math. Mech., Vol. 36, (2015), 777.
[22] M. Ayatollahi, M. M. Monfared and M. Nourazar, J. Intell. Mater. Syst. Struct., Vol. 28, (2017), 2823.
[23] R. Bagheri, M. Ayatollahi and S. M. Mousavi, Int. J. Mech. Sci., Vol. 93, (2015), 93.
[24] R.T Faal and A. A. Dehghan, Eng. Fract. Mech., Vol. 140, , (2015), 17.